Automatic Detection of Multi-Modality in Self-Mixing Interferometer

Usman Zabit, Khadija Shaheen, Maryam Naveed, Olivier Bernal, Thierry Bosch

Automatic Detection of Multi-modality in Self-Mixing Interferometer

Usman Zabit, *Member IEEE*, Khadija Shaheen, Maryam Naveed, Olivier D. Bernal, *Member IEEE* and Thierry Bosch, *Senior Member IEEE*

***Abstract*— Laser feedback based self-mixing interferometry (SMI) has been demonstrated for diverse metric sensing applications. Typically, SMI sensors are based on such laser diodes (LDs) which provide mono-modal emission resulting in SMI signals in which each interferometric fringe occurs due to change in optical path length of λ/2, where λ is emission wavelength. However, in case multiple laser modes undergo SMI, then each mode contributes its own set of fringes. As LDs can emit multiple modes under variable operating conditions, so, non-detection of multiple SMI modes can cause drastic increase in measurement error due to wrong interpretation of fringes. Previously, detection of multiple laser modes undergoing SMI was achieved by adding spectroscopic instruments to the SMI set-up. This, however, compromises the inherent simplicity of SMI sensing. In this work, an automatic SMI based multi-modality detection method is proposed which is able to detect if multiple modes of deployed LD are undergoing SMI and are contributing additional fringes within the SMI signal under variable sensing conditions. Such detection enables correct interpretation of SMI fringe count and can be used to signal occurrence of mode-hopping or secondary mode excitation. The method uses an artificial neural network, able to automatically identify uni-, bi-, or tri-modal SMI signals. Two different LDs (emitting at 637 nm and 650 nm) were used to acquire 131 experimental uni-, bi-, and tri-modal SMI signals for variable operating conditions and target vibration amplitude. The proposed system has achieved modality detection accuracy of 98.57% on 70 unseen experimental SMI signals.**

***Index Terms*— Self-mixing Interferometry, Optical Feedback Interferometry, Vibration Measurement, Laser Sensors, Neural Networks, Laser modes, Laser feedback.**

I. Introduction

Self-mixing interferometry (SMI) or optical feedback interferometry [1, 2] based laser sensors have been demonstrated for diverse sensing applications such as displacement [3, 4], distance [5], vibration [6, 7], velocity [8], refractive index [9], range finding [10], flow [11], strain [12], and imaging [13] etc.

Traditionally, mono-modal laser diodes (LD) are used for SM sensing and each interferometric SM fringe is assumed to occur for a remote target motion of λ/2, where λ is the LD wavelength. λ/2 is thus considered the basic resolution of SM sensors. However, in case of change in LD modality (e.g. switching from mono-modal to bi-, or even tri-modal emission), different individual modes [14] under SM are incoherently superimposed and a corresponding sub-periodicity appears in the SM signal [15, 16]. As a result, fringes within the multimodal SM signal need to be interpreted differently. Thus, if the LD under optical feedback exhibits multi-modal behavior during the course of continuous sensing of a remote target then the corresponding multiplicity of SMI fringes needs to be appropriately detected and classified in order to correctly retrieve the target displacement with potentially improved SMI sensor resolution [15, 17]. This multiplicity of SMI fringes, however, turns into a source of drastic increase in measurement error [16] in case failure occurs in detecting the change in multiplicity of SMI fringes. Thus, any change from uni-modal to multi-modal SMI signal (or vice-versa) needs to be automatically detected followed by appropriate fringe count interpretation. Otherwise, even advanced SMI displacement/vibration retrieval algorithms yielding high accuracy (for uni-modal SMI) [18-28] will provide erroneous measurements.

Variation can occur in LD modality [14, 17] due to change in laser diode' operating current [14] or temperature [15] while change in length of external cavity also influences the modality of the laser under optical feedback [16]. Currently, change in modality cannot be detected without introducing optical components and spectroscopic instruments into the SM sensor set-up [15]. Such introduction of additional optical components, however, compromises the inherent simplicity (see Fig. 1) of SM sensing for real-world applications.

To the best of authors' knowledge, no previous method exists for automatic detection of changes in SMI signal's modality. In this work, an artificial neural network (NN) based system has been designed to achieve automatic detection and classification of multi-modality of optical feedback based SMI signals for sensing purposes using two different laser diodes.

U. Zabit (corresponding author) was with the Department of Electrical Engineering, Riphah International University, Islamabad 44000, Pakistan. He is now with the School of Electrical Engineering and Computer Sciences, National University of Sciences and Technology, Islamabad 44000, Pakistan (e-mail:usman.zabit@seecs.nust.edu.pk).
K. Shaheen and M. Naveed graduated from the Department of Electrical Engineering, Riphah International University, Islamabad 44000, Pakistan.
O. D. Bernal and T. Bosch are with the LAAS-CNRS, Universite de Toulouse, CNRS, INPT, 31400 Toulouse, France.

DOI: 10.1109/JSEN.2018.2869771

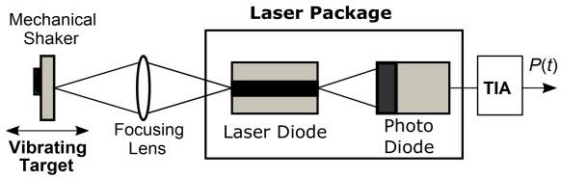

Fig. 1. Schematic diagram of SMI sensing set-up based on a laser diode package including the built-in monitor photodiode. Remote vibrating target causes variation in optical output power $P(t)$ which is detected by the monitor photodiode and amplified by a trans-impedance amplifier (TIA).

As a result, SM fringe count can now be correctly and automatically interpreted even if the SMI signal changes from uni-modal to multi-modal operation. Such a detection potentially allows the use of multi-modal lasers for sensing purposes as well, thus extending the choices in an area previously dominated by mono-modal lasers. Similarly, it enables monitoring and SMI based use of such uni-modal laser diodes which are prone to switch to multimode operation e.g. due to change in operating conditions.

As another potential use, the automatic multi-modality detection provided by the NN can also be used in a feedback loop so that either LD operating current [17] and/or the focusing lens position be electronically controlled (e.g. as already demonstrated for the robust stabilization of optical feedback regime of SMI sensor using electronically controlled liquid lens [21]) so that LD based SMI sensor is stabilized to operate with a specific uni-/multi-modal behaviour.

NNs have been regularly used to improve the performance and selectivity of various sensors such as surface acoustic wave sensor array [29], gas-mixture sensors [30], optical-fiber based sensor [31], and chemical sensors [32] etc. Likewise, NNs have also been used for SMI based sensing. For example, an SMI sensor, using NN for the data processing, was designed to classify the surface of the remote moving target [33]. The results presented better than 92% correct classification for eight different surfaces involving different materials, manufacturing methods, and roughness levels. The NN used statistics of mean speckle amplitude, mean speckle frequency, and speckle contrast [33]. Similarly, NN was used to eliminate the noise associated with the uni-modal SMI signals belonging to weak and moderate optical feedback regimes [34]. It eliminated noise by means of NN curve fitting technique. Simulations revealed a measuring accuracy of λ/25 for weak optical feedback and λ/20 for moderate optical feedback regime SMI signals [34].

The paper is organized as follows: Section II discusses the broad principles of SMI and the deployed experimental set-up for acquisition of multi-modal SMI signals. NN based classification methodology and detection results are described in Section III followed by *Discussion* and *Conclusion*.

II. Self-Mixing Interferometry

SMI is a very attractive sensing scheme in the way that it allows a simple laser diode (LD) package (containing its built-in photodiode) to be simultaneously used as a laser source, a micro-interferometer, and a detector. This thus allows a compact, miniaturized, low-cost, and self-aligned sensor capable of nanometric measurement accuracy [1-2]. An SMI system is much simpler than conventional interferometers because many optical elements such as beam splitters, reference mirror, and external photo-detector are not required. Thus, with a simply constructed optoelectronic system, smart laser sensors have been developed using SMI.

SMI signals are observed when a part of the back-reflected laser beam illuminating a remote target re-enters into the active optical cavity. This then causes a mixing of generated and back-reflected optical fields within the laser cavity. The said mixing or interference affects the properties of laser including modulation of its wavelength [14] and optical output power (OOP) of the laser as a function of changes in the optical path length [13]. The variation in the OOP of the laser diode $P(t)$ caused by this optical feedback can be written as [1]:

$$P(t) = P_0[1 + mcos[\Phi_F(t)]] \quad (1)$$

where P_0 is the emitted power under free running conditions, m is the modulation index and $\Phi_F(t)$ is the laser output phase in the presence of feedback, given by [1]:

$$\Phi_F(t) = 2\pi \frac{D(t)}{\lambda_F(t)/2} \quad (2)$$

where $D(t)$ is the target displacement. The emission wavelength subject to feedback $\lambda_F(t)$ is provided by the well-known excess phase equation [1]:

$$\Phi_0(t) = \Phi_F(t) + Csin[\Phi_F(t) + \arctan(\alpha)] \quad (3)$$

where $\Phi_0(t)$ is the laser output phase in the absence of feedback, given by:

$$\Phi_0(t) = 2\pi \frac{D(t)}{\lambda_0(t)/2} \quad (4)$$

where λ_0 is the emission wavelength under free running conditions, and α is the line width enhancement factor, also known as Henry's factor [35]. The feedback coupling factor C, also known as Acket's parameter [36], is usually used to identify the SM operating regime such as weak- ($C < 1$), moderate-($1 < C < 4.6$), or strong- ($C > 4.6$) optical feedback regime [1, 2].

A. Self-Mixing Sensing Set-up

Fig. 1 schematizes a basic arrangement for studying the SM effect. The arrangement consists of a laser diode biased with a constant current while the built-in monitor photodiode, receiving light from the back facet of the laser diode, is used to measure the optical output power emitted by the laser.

The so-called external cavity is created between the front facet of LD and moving target, which may be cooperative (i.e. mirror) or non-cooperative (i.e. diffuse surface). For a given target surface, the focusing lens placed in the external cavity and the sensor-to-remote-target distance determine the amount of optical feedback coupling into the LD.

DOI: 10.1109/JSEN.2018.2869771

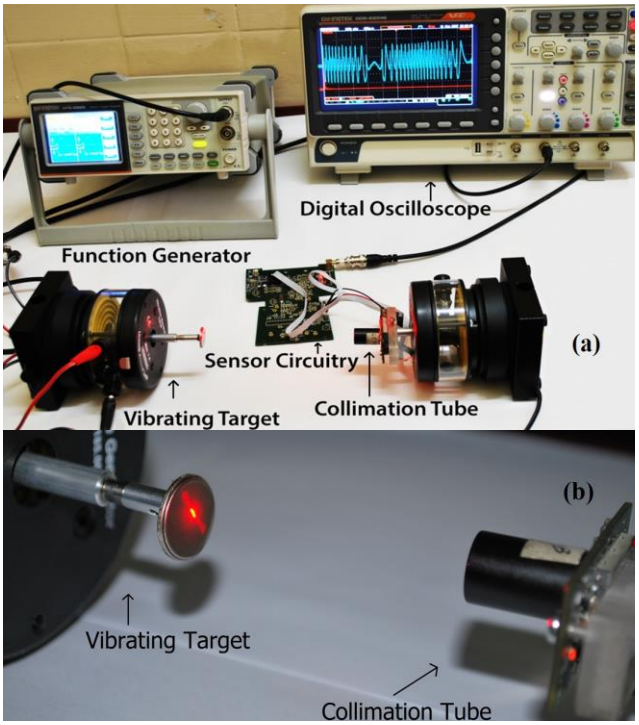

Fig. 2. (a) Experimental set-up for acquiring uni- and multi- modal self-mixing interferometric signals using two different laser diodes, (b) close-up.

B. *Experimental Set-up*

The basic SM interferometer was implemented by using the experimental set up shown in Fig. 2. The vibrating target was a polished metallic ring mounted on a mechanical shaker (model SF-9324 by PASCO having operating frequency range of about 0.1Hz to 5 kHz). The function generator (model AFG-2225 by GW Instek) provided sinusoidal input vibration of 100 Hz frequency to the wave driver. The digital oscilloscope (model GDS-2204E by GW Instek) was used to observe and to acquire the SMI signals.

The experimental setup was tested using two different LDs i.e. L637P5 and HL6501MG. L637P5 LD has threshold current I_{th} of 20mA, a slope efficiency η of 1mW/mA and λ_0 of 637nm at 25˚C, providing 5 mW of optical power. HL6501MG LD has I_{th} of 75mA, η of 0.75mW/mA and λ_0 of 650 nm at 25˚C providing 35 mW of optical power.

The collimation tube (model LT110P-B by ThorLabs) with focusing lens of 6.24 mm focal length was used to house the laser diode and to focus the laser beam onto the vibrating target. A custom-made circuit board was used to drive the LD with adjustable operating current. It also includes a trans-impedance amplifier (TIA) to amplify the photodiode signal.

C. *Experimental Observations*

The laser diode L637P5 was biased with constant current of 23mA and the external cavity length L_{ext} was about 10 cm. The lens of collimation tube was initially set to the defocus position thus small amount of optical feedback occurred resulting in a mono-modal SMI signal as shown in Fig. 3(b). When the amount of optical feedback was increased by focusing the lens, other modes of LD also entered SM and a sub-periodicity appeared in the optical output power, resulting in a bi-modal SM signal, as seen in Fig. 3(c). When the amount of optical feedback was increased further, tri-modal SMI signal appeared, as seen in Fig. 3(d).

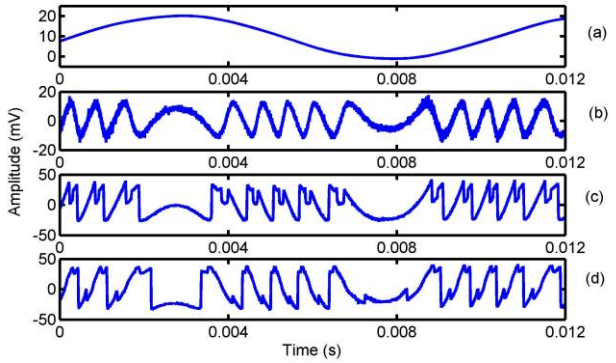

Fig. 3. Experimentally acquired SMI signals using L637P5 laser diode with operating current of 23mA. (a) driving voltage provided to the vibrating mechanical shaker acting as target, (b) mono-modal SMI signal, (c) bi-modal SMI signal, and (d) tri-modal SMI signal. Note the characteristic sub-periodicity in SMI fringes indicative of multi-modality.

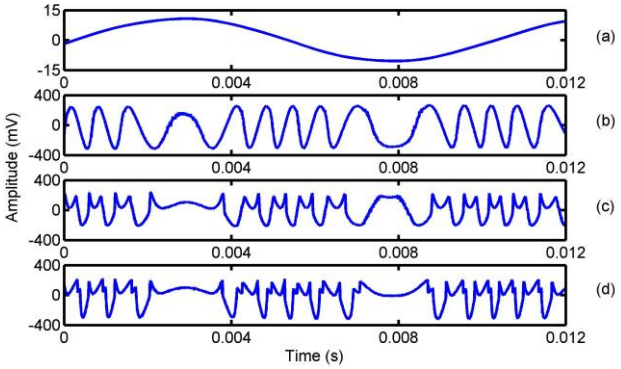

Fig. 4. Experimentally acquired SMI signals using HL6501MG laser diode with operating current of 78mA. (a) driving voltage provided to the vibrating mechanical shaker acting as target, (b) mono-modal SMI signal, (c) bi-modal SMI signal, and (d) tri-modal SMI signal.

Similar results were obtained by using HL6501MG with operating current of 78mA, as shown in Fig. 4.

It was also observed that the shape of a given multi-modal (e.g. tri-modal) SM signal significantly varied as L_{ext} was varied while the focus remained the same (see Fig. 5 and Fig. 6). This may be due to different gain and phase shifts encountered by individual modes making up the tri-modal signal which are incoherently superimposed [15, 16].

"Previous research [15] measured the optical spectra corresponding to multiple modes undergoing optical feedback. The number of modes undergoing SM was controlled by varying the amount of optical feedback (which in their experimental setup was controlled through a variable optical attenuator). Importantly, it was also experimentally observed that a normally mono-modal laser diode (such as Mitsubishi ML1412 LD with I_{th} of 43 mA, η of 0.75 mW/mA, and λ_0 of 680 nm at 25 °C) can be subject to mode hopping under optical feedback [15]. Specifically, when ML1412 LD was biased at 50 mA then it presented a mono-modal optical

DOI: 10.1109/JSEN.2018.2869771

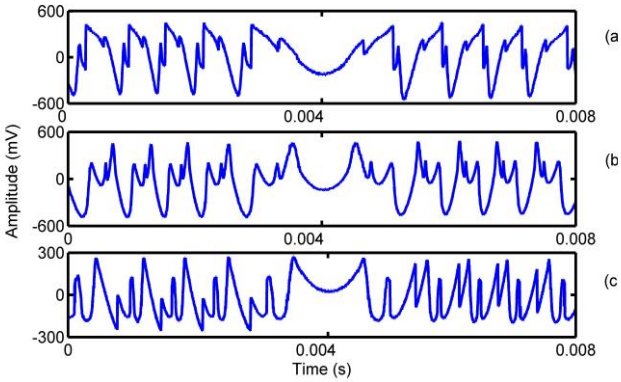

Fig. 5. Different tri-modal SMI signals observed using HL6501MG laser diode at different external cavity lengths of approx. (a) 10 cm (b) 13 cm (c) 15 cm respectively.

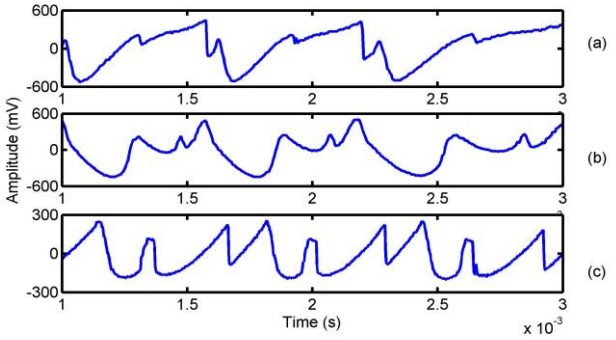

Fig. 6. Magnified portion (0.001s to 0.003s) of Fig.5 showing the variation in shape of different tri-modal SMI signals.

emission spectrum. However, under specific amount of optical feedback resulting in a bi-modal SM signal, the corresponding optical spectrum showed that optical intensity of the second mode was approximately 80% with respect to the primary mode. Likewise, in the case of tri-modal SM signal, optical intensity of second (third) mode was approximately 75% (55%) with respect to the primary mode [15]."

A variety of SMI signals were thus observed and acquired under different optical feedback and L_{ext} conditions. Weak feedback regime signals are identified by quasi-sinusoidal fringes devoid of discontinuity (e.g. see Fig. 3 (b) and Fig. 4 (b)). Moderate feedback regime signals are characterized by presence of sharp discontinuity at each fringe as well as hysteresis [1,2]. Certain acquired SM signals belong to moderate feedback regime (e.g., see Fig. 3 (c-d). Strong feedback regime SM signals are usually avoided due to fringe-loss and chaos [1, 2]. No such signals were observed during signal acquisition for the present work.

Having discussed how different mono- and multi-modal SMI signals were experimentally acquired, methodology of their automatic classification and detection is discussed next.

III. Classification of Modality

Schematic block diagram of the proposed classification and detection of mono- and multi-modal SMI signals for vibration sensing is shown in Fig. 7. It is composed of four sub-blocks: 1) SMI Data-set, 2) Pre-processing, 3) Feature Extraction, and 4) Classification, as detailed below.

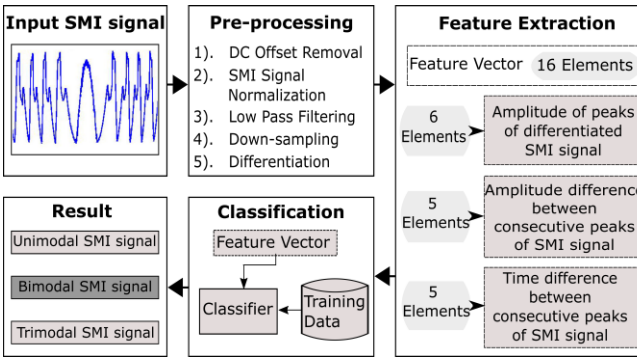

Fig. 7. Schematic block diagram of proposed automatic detection method of uni- and multi-modal SMI signals for vibration sensing.

A. SMI Data-set

As previously mentioned, various mono-, bi-, and tri-modal experimental SMI signals were acquired using two different LDs by varying the optical feedback through variation of L_{ext} (from 15 cm to 60 cm approximately) and lens' focus. The peak to peak amplitude of target vibration was also varied (from 0.7 µm to 3 µm approximately) resulting in change in the number of fringes per vibration cycle in SMI signal (varying from 2, 4, or 6 fringes to 9, 18, or 27 fringes for uni-, bi-, or tri-modal operation respectively). Thus, multiple mono-modal, bi-modal, and tri-modal SMI acquisitions were obtained to form a data-set. Specifically, this data-set is composed of 131 SMI signals with 42 uni-modal (32.1%), 42 bi-modal (32.1%), and 47 tri-modal (35.8%) SMI signals.

B. Pre-processing

Different SMI signals are made comparable by removing any dc offset followed by normalization of SMI signal amplitude within the range [1 -1]. Likewise, for correct classification, it is important to enhance the quality of the input experimental SMI signals by using filtering to reduce noise. Lastly, it is important to take such steps (e.g. differentiation) so that subsequent features can be extracted (see Fig. 8).

1) DC Offset Removal
2) SMI Signal Normalization
3) Low Pass Filtering

The normalized SMI signal is passed through a low pass filter. This improves the overall signal to noise ratio of experimentally acquired SMI signals and makes their patterns (based on sub-periodicity in case of multi-modality) become more prominent (see Fig. 8 (b)).

4) Down-sampling

DOI: 10.1109/JSEN.2018.2869771

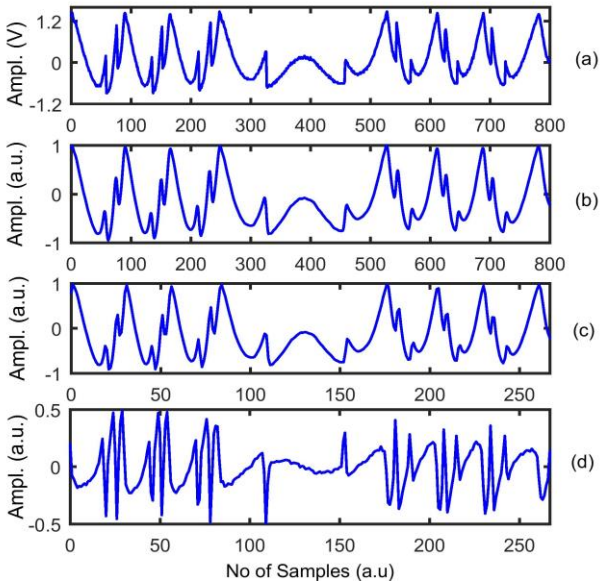

Fig. 8. Preprocessing steps: (a) raw experimentally acquired SMI signal, (b) normalized and low-pass filtered SMI signal, (c) down-sampled SMI signal, and (d) differentiated SMI signal.

The process of down-sampling is performed (by a factor of 3) thereby reducing the total number of samples of raw SMI signal which is sampled at a high sampling rate. As a result, the slopes of transitions (indicative of fringes) in SM signal become steeper and hence can be better localized in subsequent steps (see Fig. 8(c)). Note that all subsequent steps are carried out on this filtered and down-sampled SMI signal, denoted as SM_d.

5) Differentiation

The pattern of transitions (indicative of location of individual fringes) in multi-modal SMI signals is an important feature for classification of SMI multi-modality as this pattern is indicative of individual modes contributing in a multi-modal SMI signal. By performing differentiation of SM_d, each transition (fringe) within the SMI signal appears as local peak in differentiated SMI signal (see Fig. 8(d)). Thus, these transitions (indicative of individual fringes) can be localized and the associated pattern can be identified and later used as a part of other features indicative of modality.

C. Feature Extraction

As experimental SMI signals can be composed of hundreds of thousands of samples per second due to high sampling rate requirements of typical SMI signals so it is important to reduce the dimensionality of the input SM signals while preserving their significant features (whose values are different for each class of modality, thus enabling class identification). This stage is known as feature extraction. So input data is processed in such a way that the useful features (providing clues of a certain modality) existing in the SMI signal are extracted. The important features include:

1) Amplitude of peaks of differentiated SMI signal

The pattern made up by the values of amplitude of peaks in differentiated SMI signal is usually different in each case of modality of SMI signals (i.e. mono-modal, bi-modal, and tri-modal SMI signal.) These peaks, shown in Fig. 9(a), need to be first detected and then their amplitude values and locations (used later on) are saved. Values of six consecutive peaks are used later as features.

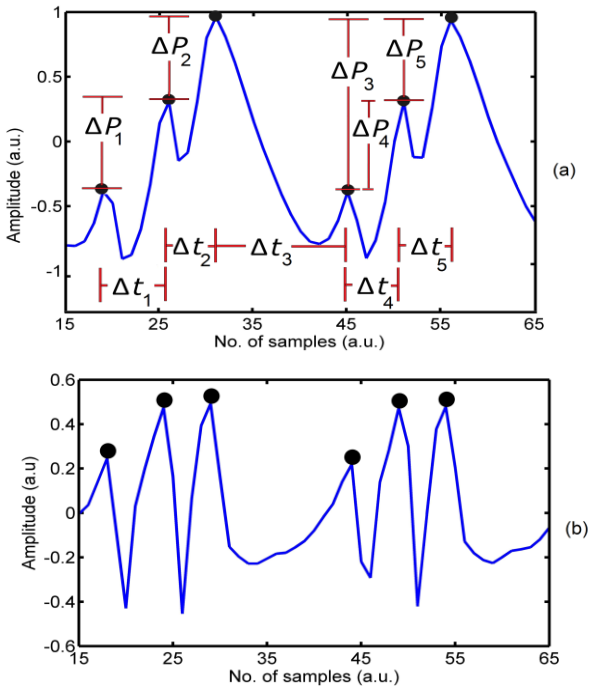

Fig. 9. (a) Fringes of a tri-modal SMI signal and corresponding detected peaks indicated by black circles. The time difference (Δt) and amplitude difference (ΔP) between consecutive peaks are also indicated. (b) Peaks of corresponding differentiated SMI signal indicated by black circles.

2) Amplitude difference between consecutive peaks

The peaks of SM_d signal are identified and the difference of amplitude (ΔP) between 6 consecutive peaks (resulting in five ΔP values) is computed as shown in Fig. 9. The pattern of ΔP is usually different in each mode of SMI signal and thus can be utilized for modality classification.

3) Time difference between consecutive peaks

The time indices of peaks in SM_d signal are identified (using their location information) and the difference of indices (Δt) between 6 consecutive peaks (resulting in five Δt values) are computed as shown in Fig. 9. The pattern of Δt is also usually different in each mode of SMI signal which makes it a useful feature.

In order to achieve high accuracy in modality classification, following guidelines were followed:

1) The detected peaks should not include the direction-reversal segment of SMI signal, as it is devoid of true fringes.

2) No genuine peak should remain undetected within the SMI signal segment used for feature extraction."

Thus, each SMI signal is processed so that its corresponding feature vector is obtained. The feature vector is then composed of 16 total elements in which 6 elements are taken from the peak value of differentiated SMI signal, 5 elements from the amplitude difference between peaks of SM_d, and 5 elements from time difference between peaks of SM_d. All such feature

DOI: 10.1109/JSEN.2018.2869771

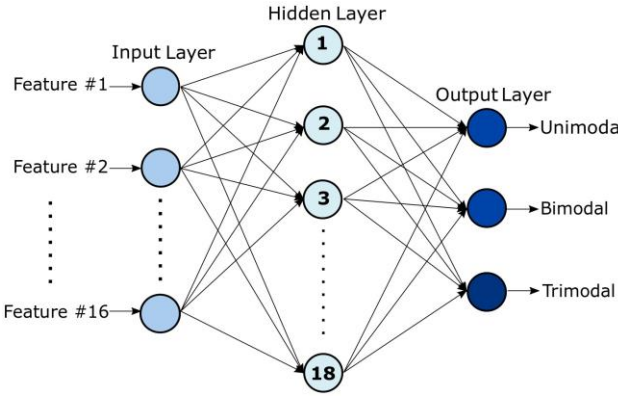

Fig. 10. The architecture of neural network employed for the proposed classification of multi-modality in SMI signals for vibration sensing.

vectors of complete data-set are then passed on to the NN for supervised classification, as detailed below.

D. Classification

1) Supervised learning

For supervised learning, the training data is provided to the classifier. The training data is composed of extracted feature vectors of different uni-, and multi-modal SMI signals and the corresponding output labels. The output label represents classes of SM signals, i.e. class U, B, or T corresponding to uni-, bi-, or tri- modal SMI signal respectively. In our case, 61 labeled SMI signals out of the 131 total SMI signals have been used for training of classifier.

The neural network pattern recognition MATLAB ® toolbox is used as classifier. This classifier not only creates a NN but also validates its performance after supervised learning. This classifier is using back propagation algorithm for training of NN. The architecture of employed NN is shown in Fig. 10 in which the input layer is composed of 16 nodes (each receiving one input from the SMI feature vector), the output layer has three elements (each indicating the detected SMI modality, i.e. U (for uni-modal), B (for bi-modal), and T (for tri-modal)) while there is one hidden layer comprising of 18 neurons.

2) Testing of Classification

After the training of NN, it is used to classify the unseen and unlabeled SMI signals into one of three modal classes. The unseen and unlabeled SMI signal is passed through preprocessing stage and features are extracted from it. The feature vector is provided as input to the trained classifier and then it makes the decision about its class with a certain performance, as detailed below.

TABLE I
DETECTION PERFORMANCE OF NEURAL NETWORK FOR UNSEEN SMI UNI-, BI-, AND TRI-MODAL SIGNALS AS A FUNCTION OF NUMBER OF NEURONS

Number of Hidden Neurons	Modality Detection Performance for Unseen SM Signals				
	Uni-modal signals	Bi-modal signals	Tri-modal signals	Total SM signals	Accuracy (%)
16	21/22	21/22	23/26	65/70	92.85
18	22/22	22/22	25/26	69/70	98.57
20	22/22	21/22	24/26	67/70	95.71
22	22/22	22/22	22/26	66/70	94.28

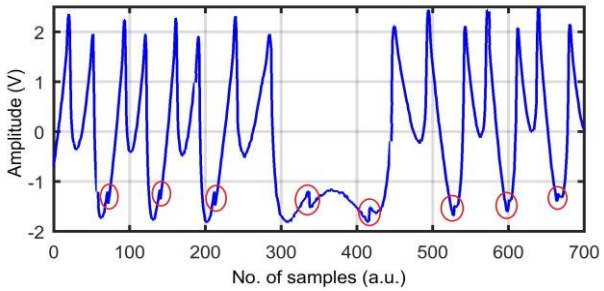

Fig. 11. The only incorrectly classified unseen SM signal is a tri-modal SM signal which was classified as a uni-modal SM signal by the NN. Very small SMI fringes of the third mode are encircled in red near -1.3 V.

E. Results

The performance of proposed NN is quantified by computing its accuracy of classification. Here, accuracy is the ratio of correctly classified SMI signals to total number of SMI signals that are being classified.

The results of classification are shown in Table I. The proposed NN was provided 70 unseen SMI signals (composed of 22 uni-modal, 22 bi-modal, and 26 tri-modal SMI signals). The NN has provided best results when 18 neurons are used in the hidden layer. In this case, the classifier performed correct SM modality detection on 69 out of 70 unseen uni-, and multi-modal SMI signals with 98.57% overall correct detection accuracy.

IV. DISCUSSION

The number of neurons N_{hl} in the hidden layer of the neural network affects the performance in terms of correct detection of modality of SMI signals. As seen in Table I, if $N_{hl} \leq 16$ then the performance of NN will comparatively decrease as it will not be able to make use of all 16 input features. On the other hand, if $N_{hl} > 18$, then comparatively poorer performance is attained due to data over-fitting problem. So, for the proposed scheme, best SM modality classification accuracy of 98.57% was obtained when 18 hidden neurons are used inside the NN.

It is also seen in Table I that the NN is able to successfully detect all unseen uni-modal SM signals. Such a result is to be expected given the observation that uni-modal SM signals are the least diverse in nature as compared to bi-, or tri-modal SM signals. Performance of the NN in detecting unseen bi-modal signals is also very good due to appropriate choice of features and pre-processing.

Focusing on the incorrect detection by the NN, it can be noted in Fig. 11 that such a tri-modal SM signal is quite difficult to correctly classify due to very small amplitude of the third mode contained in this signal (see very small fringes belonging to the third mode (encircled in red) at around -1.3 V in Fig. 11). Furthermore, the other two modes of this signal (and their derivative peaks) not only have comparable amplitudes but are also evenly placed in time. This special relationship between the dominant two modes leads to a pattern similar to that of typical uni-modal SMI signals (and the NN mis-classified this signal as a uni-modal signal). This

DOI: 10.1109/JSEN.2018.2869771

signal thus exemplifies the remaining challenges in achieving 100% multi-modality detection, and is the limiting case of the proposed method.

Previous research on multimodal SMI indicated presence of up to three modes [14-17]. In case more than 3 modes undergo SMI then the proposed method could be modified to detect additional modes as well. However, the total number of input features to the NN would need to be increased to capture the variations contained in additional mode(s). E.g., if four modes undergo SMI then number of input features would need to be increased from 16 at present to 22.

V. Conclusion

Automatic detection and classification of uni-, and multi-modal self-mixing interferometric vibration sensor signals has been achieved by using a NN based method. This has been achieved through appropriate feature extraction and training of the NN. This technique has successfully processed various experimentally acquired noisy SMI signals (acquired using two different laser diodes emitting at 637 nm and 650 nm respectively) as a function of their multimodality. The three classes of multimode SMI signals (uni-modal, bi-modal, and tri-modal SMI signal) were classified with 98.57% overall correct recognition, with 100 %, 100%, and 96.15% correct detection of uni-, bi-, and tri-modal SMI signals respectively.

The detection of multimodality of SMI signals is of high significance in order to enable the use of multi-modal SM signals for metric sensing purposes while such an automated detection of SMI multimodality, to the best of our knowledge, has not been achieved before.

This signal processing based automatic identification of change in modality of a laser diode operating under different optical conditions is a significant challenge and has important repercussions on the error performance of the SM sensor. As stated previously, this has not been achieved before, thereby, 1) restricting the use of multimodal lasers (potentially providing higher SM sensing resolution [15]) for robust SM sensing set-ups or 2) restricting the use of uni-modal laser diodes having a risk of switching to multimode operation under SM e.g. due to change in operating conditions. The number of laser modes of a unimodal or multi-modal laser can vary due to operating conditions [16, 17]. Therefore, previously, it has been difficult (without adding bulky and expensive optical spectroscopic instruments into optical path thus destroying the simplicity of SM sensing set-up) to ascertain as to how many modes are lasing under SM conditions. As each mode would engender its own set of interferometric fringes, therefore, an unidentified change in modality of SM sensor can greatly affect the total fringe count thus greatly undermining the SM sensor performance as each interferometric fringe is usually assumed to identify $\lambda/2$ displacement under uni-modal SM sensing. The proposed NN based identification of multi-modality can thus potentially pave the way for the increased use of multi-modal SM sensors under varying operating and optical feedback conditions.

Likewise, the automatic modality detection enabled by the designed NN can also be used in a feedback loop (involving LD current control [17] and/or the focusing lens' electronic control [21]) so that the SMI sensor could be stabilized to operate with a specific uni-/multi-modal behaviour.

Future work would focus on improved detection performance by using additional features of multi-modal SM signals while real-time implementation involving active feedback loop would also be considered. More SM signals belonging to diverse laser sources and optical conditions can also be added to form a bigger data bank to improve the reliability of NN based modality detection over time.

References

[1] S. Donati, "Developing self-mixing interferometry for instrumentation and measurements," *Laser & Photonics Reviews*, vol. 6, pp. 393-417, 2012.

[2] T. Taimre, M. Nikolić, K. Bertling, Y. L. Lim, T. Bosch, and A. D. Rakić, "Laser feedback interferometry: A tutorial on the self-mixing effect for coherent sensing," *Advances in Optics and Photonics*, vol. 7, pp. 570-631, 2015.

[3] I. Milesi, M. Norgia, P. P. Pompilio, C. Svelto, and R. L. Dellaca, "Measurement of local chest wall displacement by a custom self-mixing laser interferometer," *IEEE Transactions on Instrumentation and Measurement*, vol. 60, pp. 2894-2901, 2011.

[4] O. Bernal, H. C. Seat, U. Zabit, F. Surre, and T. Bosch, "Robust Detection of Non Regular Interferometric Fringes from a Self-Mixing Displacement Sensor using Bi-Wavelet Transform," *IEEE Sensors Journal*, vol. 16, p. 7903, 2016.

[5] M. Norgia, G. Giuliani, and S. Donati, "Absolute distance measurement with improved accuracy using laser diode self-mixing interferometry in a closed loop," *IEEE transactions on Instrumentation and Measurement*, vol. 56, pp. 1894-1900, 2007.

[6] L. Lu, W. Zhang, B. Yang, J. Zhou, H. Gui, and B. Yu, "Dual-channel self-mixing vibration measurement system in a linear cavity fiber laser," *IEEE Sensors Journal*, vol. 13, pp. 4387-4392, 2013.

[7] Z. A. Khan, U. Zabit, O. D. Bernal, M. O. Ullah, and T. Bosch, "Adaptive Cancellation of Parasitic Vibrations Affecting a Self-Mixing Interferometric Laser Sensor," *IEEE Transactions on Instrumentation and Measurement*, vol. 66, pp. 332-339, 2017.

[8] A. Valavanis, P. Dean, Y. L. Lim, R. Alhathlool, M. Nikolic, R. Kliese, *et al.*, "Self-mixing interferometry with terahertz quantum cascade lasers," *IEEE Sensors Journal*, vol. 13, pp. 37-43, 2013.

[9] Y. Zhang, Y. Wei, C. Chen, W. Huang, X. Wang, and H. Xu, "Self-Mixing Interferometer Based on Frequency Analysis Method for Accurate Refractive Index Measurement," *IEEE Photonics Journal*, vol. 8, pp. 1-6, 2016.

[10] M. Norgia, A. Magnani, and A. Pesatori, "High resolution self-mixing laser rangefinder," *Review of Scientific Instruments*, vol. 83, p. 045113, 2012.

[11] M. Norgia, A. Pesatori, and L. Rovati, "Self-mixing laser Doppler spectra of extracorporeal blood flow: a theoretical and experimental study," *IEEE Sensors Journal*, vol. 12, pp. 552-557, 2012.

[12] M. Suleiman, H. C. Seat, and T. Bosch, "Interrogation of fiber Bragg grating dynamic strain sensors by self-mixing interferometry," *IEEE Sensors journal*, vol. 8, pp. 1317-1323, 2008.

DOI: 10.1109/JSEN.2018.2869771

[13] K. Bertling, J. Perchoux, T. Taimre, R. Malkin, D. Robert, A. D. Rakić, *et al.*, "Imaging of acoustic fields using optical feedback interferometry," *Optics express*, vol. 22, pp. 30346-30356, 2014.

[14] J. Keeley, J. Freeman, K. Bertling, Y. L. Lim, R. A. Mohandas, T. Taimre, *et al.*, "Measurement of the emission spectrum of a semiconductor laser using laser-feedback interferometry," *Scientific Reports*, vol. 7, p. 7236, 2017.

[15] M. Ruiz-Llata and H. Lamela, "Self-mixing technique for vibration measurements in a laser diode with multiple modes created by optical feedback," *Applied optics*, vol. 48, pp. 2915-2923, 2009.

[16] J. R. Tucker, A. D. Rakić, C. J. O'Brien, and A. V. Zvyagin, "Effect of multiple transverse modes in self-mixing sensors based on vertical-cavity surface-emitting lasers," *Applied Optics*, vol. 46, pp. 611-619, 2007/02/01 2007.

[17] T. Pham, H. Seat, O. Bernal, F. Surre, and T. Bosch, "Self-mixing sensing under strong feedback using multimode semiconductor lasers," in *Lasers and Electro-Optics Pacific Rim (CLEO-PR), 2013 Conference on*, 2013, pp. 1-2.

[18] A. L. Arriaga, F. Bony, and T. Bosch, "Real-time algorithm for versatile displacement sensors based on self-mixing interferometry," *IEEE Sensors Journal*, vol. 16, pp. 195-202, 2016.

[19] O. D. Bernal, U. Zabit, and T. Bosch, "Study of laser feedback phase under self-mixing leading to improved phase unwrapping for vibration sensing," *IEEE Sensors Journal*, vol. 13, pp. 4962-4971, 2013.

[20] Z. Wei, W. Huang, J. Zhang, X. Wang, H. Zhu, T. An, *et al.*, "Obtaining Scalable Fringe Precision in Self-Mixing Interference Using an Even-Power Fast Algorithm," *IEEE Photonics Journal*, vol. 9, pp. 1-11, 2017.

[21] O. D. Bernal, U. Zabit, and T. M. Bosch, "Robust method of stabilization of optical feedback regime by using adaptive optics for a self-mixing micro-interferometer laser displacement sensor," *IEEE Journal of Selected Topics in Quantum Electronics*, vol. 21, pp. 336-343, 2015.

[22] A. Ehtesham, U. Zabit, O. Bernal, G. Raja, and T. Bosch, "Analysis and Implementation of a Direct Phase Unwrapping Method for Displacement Measurement using Self-Mixing Interferometry," *IEEE Sensors Journal*, vol. 17, pp. 7425-7432, 2017.

[23] S. Donati, D. Rossi, and M. Norgia, "Single Channel Self-Mixing Interferometer Measures Simultaneously Displacement and Tilt and Yaw Angles of a Reflective Target," *IEEE Journal of Quantum Electronics*, vol. 51, pp. 1-8, 2015.

[24] Y. Fan, Y. Yu, J. Xi, and J. F. Chicharo, "Improving the measurement performance for a self-mixing interferometry-based displacement sensing system," *Applied Optics*, vol. 50, pp. 5064-5072, 2011.

[25] G. Giuliani, S. Bozzi-Pietra, and S. Donati, "Self-mixing laser diode vibrometer," *Measurement Science and Technology*, vol. 14, p. 24, 2002.

[26] A. A. Siddiqui, U. Zabit, O. D. Bernal, G. Raja, and T. Bosch, "All Analog Processing of Speckle Affected Self-Mixing Interferometric Signals," *IEEE Sensors Journal*, vol. 17, pp. 5892-5899, 2017.

[27] A. Jha, F. J. Azcona, and S. Royo, "Frequency-Modulated Optical Feedback Interferometry for Nanometric Scale Vibrometry," *IEEE Photonics Technology Letters*, vol. 28, pp. 1217-1220, 2016.

[28] A. Magnani, A. Pesatori, and M. Norgia, "Self-mixing vibrometer with real-time digital signal elaboration," *Applied Optics*, vol. 51, pp. 5318-5325, 2012.

[29] S. K. Jha and R. Yadava, "Preprocessing of SAW sensor array data and pattern recognition," *IEEE Sensors Journal*, vol. 9, pp. 1202-1208, 2009.

[30] L. Zhao, X. Li, J. Wang, P. Yao, and S. A. Akbar, "Detection of formaldehyde in mixed VOCs gases using sensor array with neural networks," *IEEE Sensors Journal*, vol. 16, pp. 6081-6086, 2016.

[31] D. King, W. B. Lyons, C. Flanagan, and E. Lewis, "An optical-fiber sensor for use in water systems utilizing digital signal processing techniques and artificial neural network pattern recognition," *IEEE Sensors Journal*, vol. 4, pp. 21-27, 2004.

[32] J. Lozano, J. P. Santos, M. Aleixandre, I. Sayago, J. Gutierrez, and M. C. Horrillo, "Identification of typical wine aromas by means of an electronic nose," *IEEE Sensors Journal*, vol. 6, pp. 173-178, 2006.

[33] S. Shinohara, S. Ito, S. Takamiya, and H. Yoshida, "Compact optical instrument for surface classification using self-mixing interference in a laser diode," *Optical Engineering*, vol. 40, pp. 38-43, 2001.

[34] L. Wei, J. Chicharo, Y. Yu, and J. Xi, "Pre-processing of signals observed from laser diode self-mixing intereferometries using neural networks," in *Intelligent Signal Processing, 2007. WISP 2007. IEEE International Symposium on*, 2007, pp. 1-5.

[35] C. Henry, "Theory of the linewidth of semiconductor lasers," *IEEE Journal of Quantum Electronics*, vol. 18, pp. 259-264, 1982.

[36] G. Acket, D. Lenstra, A. Den Boef, and B. Verbeek, "The influence of feedback intensity on longitudinal mode properties and optical noise in index-guided semiconductor lasers," *IEEE Journal of Quantum Electronics*, vol. 20, pp. 1163-1169, 1984.

DOI: 10.1109/JSEN.2018.2869771